Biophysical Chemistry 7 (1978) 253–268

POTENTIAL AND STRUCTURE CONTROLLED INTERFACIAL BEHAVIOR OF URACIL DERIVATIVES

Viktor BRABEC, Sherril D. CHRISTIAN and Glenn DRYHURST
Department of Chemistry, University of Oklahoma, Norman, Oklahoma 73019, USA

Received 15 February 1977

The adsorption and related interfacial behavior of uracil, various methylated uracil derivatives, uridine, uridine-5'-monophosphate and uridine-3'5'-cyclic monophosphate has been studied by surface electrochemical measurements at a mercury electrode. All uracil derivatives exhibit an initial "dilute" adsorption region where the virtually flat uracil residue is adsorbed flat on the electrode surface. In the case of uracil and its methylated derivatives the area occupied by one molecule is about 60–70 A^2. Uracil, thymine and 1,5-dimethyluracil exhibit a second adsorption region where they rearrange on the surface and adopt a perpendicular orientation and occupy about 40 A^2 per molecule. In this perpendicular orientation the uracils are bound to the electrode through the N(3)-H or perhaps N(1)-H functions in a manner similar to their Watson–Crick bonding in nucleic acids. When in the perpendicular orientation the adsorbed molecules undergo extensive stacking (association) interactions, again similar to those observed between adjacent bases in nucleic acids. The ability of a uracil derivative to undergo a surface reorientation is critically dependent on electrode potential, bulk-solution concentration and molecular structure.

1. Introduction

A considerable body of theoretical and experimental evidence suggests that in many instances the biological role of biopolymers, such as polynucleotides, may be related to the adsorption and other interfacial behavior of these molecules at charged biological interfaces. At such interfaces a combination of adsorption and intermolecular association processes along with structural or conformational transitions may be the important controlling influences on biopolymers and other biomolecules.

The surfaces of mammalian cells and other biological membranes carry an appreciable electrical potential. The electrical double-layer formed in the immediate vicinity of a charged membrane-biological fluid interface may be regarded as essentially identical to that formed at an electrode surface-electrolyte solution interface [1]. Indeed, the biological membrane-biological fluid interface may be regarded as quite analogous to an electrode-electrolyte solution interface [2–7]. The potential of a cell membrane, for example, is known to alter when processes such as cell regeneration occur [8], or often, when a cell becomes malignant particularly at the time of mitosis [9–11]. In addition, when tissue is damaged a potential of injury, of somewhat obscure origin, develops at the site of trauma. This potential is clearly related to the ability of an organism to regenerate tissue or to form scar tissue [12,13].The electric fields in the immediate vicinity of, for example, a cell surface are probably very large (10^5–10^7 V cm^{-1}) although they extend over only very small distances (ca. 10–100 Å). Such intense electric fields have been shown to induce structural transitions in natural and biosynthetic polynucleotides [14–16]. In addition, the magnitude and distribution of these electric fields are very similar to those which exist at an electrode surface-electrolyte solution interface [1]. Work reported by Field et al. [17] and Schell [18] indicates that adsorption of certain polynucleotides and the related interfacial behavior at a cell surface results in manifestation of a variety of biological effects including interferon formation.

Because a charged cell surface-biological fluid interface is similar to a charged electrode surface-electrolyte solution interface, it seems reasonable that an un-

derstanding of the interfacial behavior of biomolecules at the latter interface might reveal significant information regarding the expected behavior of these molecules at biological interfaces. Recently, Brabec and Paleček [19] reported on an investigation of the adsorption of double-stranded DNA, RNA and various homopolynucleotide parts at a mercury electrode, particularly with respect to conformational changes that could be induced in these polynucleotides as a function of electrode potential. These workers interpreted their results to indicate that at potentials around −1.2 V versus SCE the adsorbed polynucleotides underwent a conformational change similar to denaturation.

We have also been interested in understanding the interfacial behavior of natural and biosynthetic polynucleotides at electrode surfaces. However, rather than beginning our investigations with these complex macromolecular species, we have begun by studying the interfacial behavior of the fundamental building blocks of nucleic acids, i.e., bases, nucleosides and nucleotides.

Previous reports from this laboratory have revealed that adenine, deoxyadenosine and deoxyadenosine mononucleotides are adsorbed at a mercury electrode with the adenine moiety adsorbed in a flat orientation and with any substituent deoxyribose or deoxyribosephosphate tilted away from the electrode surface [20]. Thus, the area occupied by one adenine molecule at the electrode surface is close to 55 $Å^2$, deoxyadenosine occupies the same area, while dAMP, dADP and dATP occupy only 70–80 $Å^2$. The area occupied by one molecule of thymine is also 55 $Å^2$ which again corresponds to the area expected for a thymine molecule adsorbed flat on the electrode surface [21]. The area occupied by thymidine, TMP, TDP and TTP ranges from 100 to 200 $Å^2$ which suggest that an appreciable fraction of the electrode surface is covered by deoxyribose or deoxyribosephosphate. In this respect the adenine and thymine series exhibit significantly different interfacial behavior.

We have recently reported that uracil, the complementary base of adenine in RNA, is also adsorbed in a flat orientation on the electrode surface and occupies an area of 63 $Å^2$ [22].

In the case of adenine, deoxyadenosine, thymine and uracil at pH 8–9 previous reports [20,21] were concerned only with the so-called "dilute" adsorption region. This is a region of concentrations where normal, easily interpretable differential capacitance versus potential (C versus E) curves are observed. However, at higher concentrations these four compounds exhibit a very well defined anomalous capacitance pit for which interpretation of C versus E curves was not possible. We have suggested in the case of adenine and deoxyadenosine that the formation of such anomalous capacitance pits is due to a surface reorientation process, although without much supporting evidence [23].

This report is concerned with the interfacial behavior of uracil and a number of its derivatives at a mercury electrode at pH 8.0. This study provides evidence that uracil and certain of its derivatives are adsorbed at the electrode-solution interface in more than one orientation, the surface orientation being critically controlled by the electrode potential, the bulk-solution concentration and structure of the uracil species.

2. Experimental

2.1. Chemicals

Chemicals were obtained from the sources indicated. Uracil (Sigma), 1-methyluracil, 3-methyluracil, 1,3-dimethyluracil and 1,5-dimethyluracil (Vega-Fox), thymine and uridine (Nutritional Biochemical), uridine-5′-monophosphate and uridine-3′,5′-cyclic phosphate (Calbiochem).

All measurements were performed in 0.5 M sodium fluoride with 0.01 M sodium phosphate (Na_2HPO_4) buffer, pH 8.0. The appropriate uracil derivative was weighed directly into this supporting electrolyte solution and, after dissolution, deaerated with water-saturated nitrogen before study.

2.2. Differential capacitance measurements

Differential capacitance measurements were obtained by a phase-selective a.c. polarographic method described previously [20–23]. The siliconized [24] dropping mercury electrode (DME) had a flow rate at open circuit of 1.930 mg s^{-1}.

The measured value of the differential capacitance per unit area at fixed frequency at different times in the drop life was found to be constant at times between <1 to >10 s over the entire range of poten-

tials studied for all compounds even with the most dilute solutions employed, i.e., d.c. equilibrium was rapidly established. All measurements were made with a controlled droptime of 2.00 s.

Between 10–250 Hz and with a 10 mV peak-to-peak amplitude for the modulating voltage, the measured capacitance was independent of frequency over the entire range of interest. Because of the absence of any significant frequency dispersion all capacity data reported here were measured at 100 Hz and 10 mV peak-to-peak.

The d.c. potential was scanned at a sweep rate of 0.005 V s^{-1}. Alternating current versus potential curves and alternating current versus time curves were recorded on a Texas Instrument Model 341 X-Y recorder or a Tektronix Model 5031 storage oscilloscope.

2.3. Direct interfacial tension measurements

Interfacial tension of a mercury electrode was measured by the maximum bubble pressure technique. The apparatus for such measurements utilized a siliconized J-shaped capillary having a radius at its tip of 0.0041 cm. The basic design of the apparatus was similar to that used by Hansen et al. [25] and has been described extensively elsewhere [22]. A Brinkman/Wenking Model LT73 potentiostat was employed. The cell for maximum bubble pressure (and differential capacitance) measurements was water jacketted and maintained at 25 ± 0.1°C.

The procedure utilized to calibrate the maximum bubble pressure apparatus and to take interfacial tension measurements has been described in detail elsewhere [22]. All potentials in this report are referred to the saturated calomel electrode (SCE) at 25°C.

3. Results

3.1. Differential capacitance and interfacial tension measurements on uracil and uracil derivatives

The analysis of capacitance results can be understood by reference to fig. 1A which shows a typical set of capacitance versus potential (C versus E) curves for uracil at pH 8.0 between −0.1 V and −1.9 V. At uracil concentrations up to about 24 mM there is a general depression of capacitance, compared to pure background electrolyte, between about −0.2 V and −0.7 V with a broad adsorption/desorption peak at more negative potentials. At uracil concentrations at or above 24 mM a very sharply defined anomalous capacitance pit is formed centered at −0.55 V. With increasing uracil concentration the depth of the capacitance pit remains invariant although it grows wider (fig. 1A). Similar anomalous capacitance pits were observed for thymine (5-methyluracil) (fig. 1B) and 1,5-dimethyluracil (fig. 1C). None of the other compounds studied (1-methyluracil, 3-methyluracil, 1,3-dimethyluracil, uridine, uridine-5′-monophosphate, cyclic uridine-3′,5′-phosphate) gave rise to capacitance pits at pH 8 even in saturated solutions. Thus the latter group of compounds gave C versus E curves which were similar to, for example, uracil at concentrations below 24 mM.

Interpretation of capacitance data could not be carried out in regions where the anomalous capacitance pits occur [20–22]. Accordingly, two adsorption regions may be defined: A "dilute" adsorption region which is observed for all compounds and which corresponds, in the case of uracil, thymine and 1,5-dimethyluracil, to concentrations where no capacitance pit is observed. The second region corresponds to concentrations where the capacitance pit is observed for uracil, thymine and 1,5-dimethyluracil.

In the dilute adsorption region all compounds gave C versus E curves which coincided with the background electrolyte curve at potentials of about −1.6 V or more negative. Accordingly, for concentrations corresponding to the dilute adsorption region the back-integration method of Grahame et al. [26] was utilized to calculate the charge of the mercury-electrolyte solution interface. Thus

$$q - q^* = \int_{E^*}^{E} C \, dE , \qquad (1)$$

where q is the charge relative to q^*, the charge at the potential, E^*, where the integration was started (E^* was usually −1.8 V). The value of the electrocapillary maximum potential (ECM) or potential of zero charge for the background electrolyte solution, measured by the maximum bubble pressure technique (vide infra), was found to be −0.433 V. At the ECM in the pure background electrolyte solution $q = 0$. Hence it is easy to calculate the absolute charge for the background

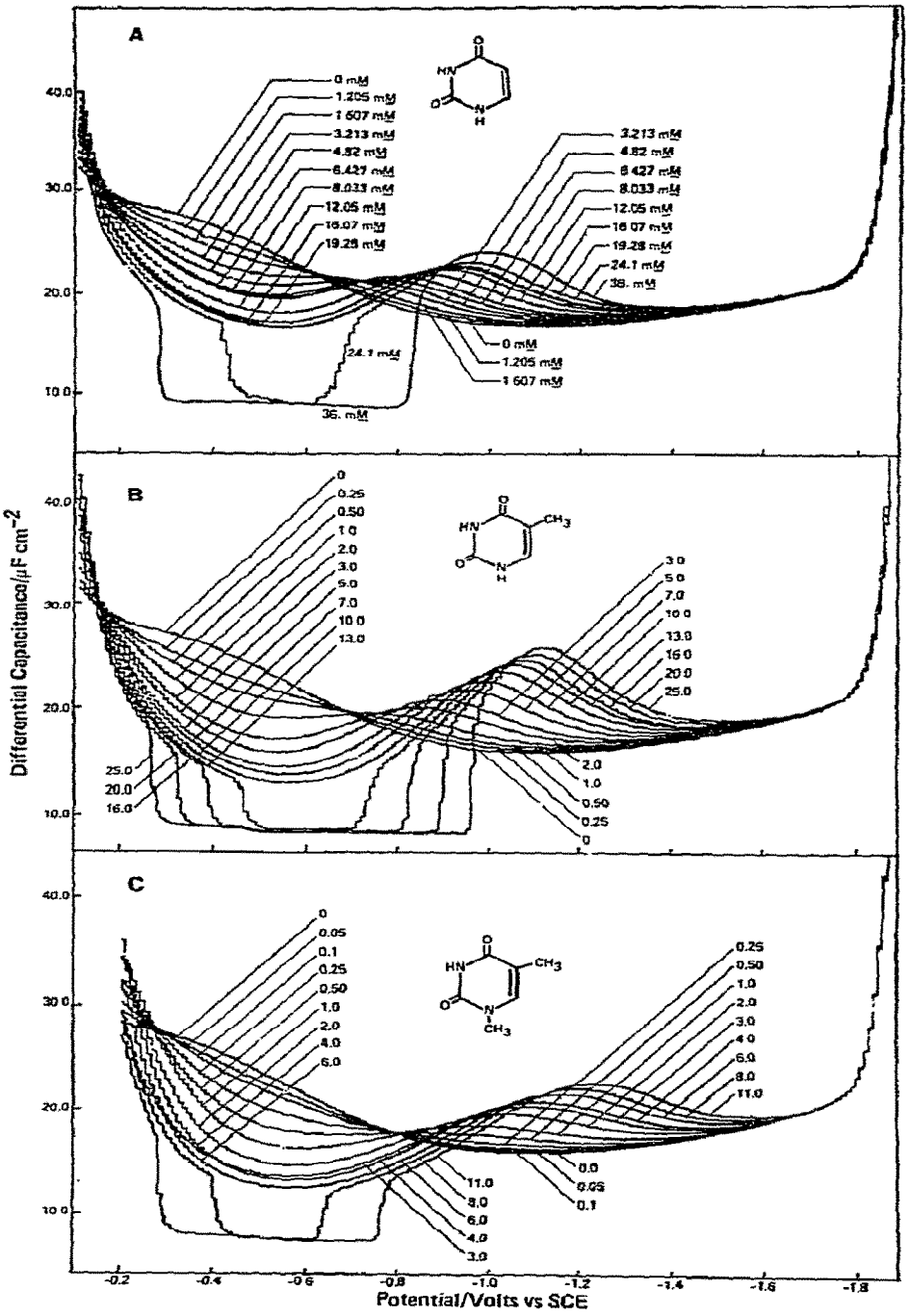

Fig. 1. Typical differential capacitance versus potential curves for (A) uracil, (B) 5-methyluracil (thymine) and (C) 1,5-dimethyluracil in 0.5 *M* NaF plus 0.01 *M* Na_2HPO_4 buffer pH8. Curves were obtained at a frequency of 100 Hz and an amplitude of 10 mV peak-to-peak. Concentrations are shown in the figure.

solution at E^*. At E^* all C versus E curves were coincident with the background curve; hence it may be concluded that the charge values, q^*, for all solutions at E^* are the same [26]. Accordingly, the values of $q - q^*$ in eq. (1) are readliy converted to absolute charge values as a function of both E and a, the activity of the uracil derivative. A further integration of charge was then carried out to obtain interfacial tension, i.e.,

$$\gamma = \gamma_0 - \int_0^E q \, dE . \qquad (2)$$

The value of γ_0, the interfacial tension for the pure background solution at the ECM was obtained directly from maximum bubble pressure measurements. Eq. (2) was used to obtain interfacial tension as a function of both E and a.

Interfacial tension data were also measured directly by means of the maximum bubble pressure technique [22]. The latter technique was used in preference to the more conventional capillary electrometer method because interfacial tension data obtained by measurements with the capillary electrometer were at variance with integrated capacitance results particularly at potentials at or more positive than the ECM [22,27,28].

3.2. Dilute adsorption region

In the dilute adsorption region the first step in analysis of interfacial tension results obtained from double integration of C versus E data or, directly, from maximum bubble pressure measurements was to calculate the surface spreading pressure, π, as a function of the uracil derivative activity, a, and electrode potential, E, using the equation

$$\pi = \gamma_w(E) - \gamma(E) , \qquad (3)$$

where γ_w is the value of γ for the pure background electrolyte solution at $a = 0$.

Concentrations of each uracil derivative were taken as equal to activity throughout this study.

Plots of surface spreading pressure, π, versus the logarithm of the activity of each uracil derivative were all readily superimposable by abscissa translation. Some representative plots are presented in fig. 2. Similar plots for uracil and thymine have been presented elsewhere [21,22]. The calculated curves in fig. 2 represent the least squares fit of π, a and E data to the empirical equation [22].

$$\pi = A[\ln(1 + Ba)]\left[1 + \frac{\alpha a}{(1 + Ba)^2} + \frac{\beta a}{(1 + Ba)^3} + \ldots\right] . \qquad (4)$$

In this equation A is equal to $\Gamma_m RT$ where Γ_m is the surface excess of the uracil derivative at $\theta = 1$, where θ is the fractional surface coverage of the electrode. The parameter B is dependent on potential so that if data are to be fitted simultaneously at several different potentials, separate B values must be inferred at each potential. A non-linear least squares procedure [29] is employed to obtain optimum values of all parameters. A detailed description of the use of eq. (4) has been presented elsewhere [21,22].

Once a composite fit had been obtained for π and a data at several potentials for a particular uracil derivative the same functional form was used to fit data at fixed potentials typically between about −0.3 V and −1.2 V. Because such very good composite π versus $\ln a$ plots were obtained it was assumed that at all potentials the value of $\Gamma_m RT$ (or A in eq. (4)) was constant. This constant value of A was used in fitting π and a data at individual potentials. Analytical differentiation of the π versus $\ln a$ fits of curves at individual potentials was used to calculate values of ΓRT at various concentrations and potentials using the Gibbs equation (eq. 5).

$$\Gamma = \frac{1}{RT} \frac{d\pi}{d \ln a} . \qquad (5)$$

Superimposability of π versus $\ln a$ plots such as those shown in fig. 2 has been widely employed to prove congruence of organic electrosorption isotherms with respect to potential. However, the validity of this test of congruence has been seriously questioned by Parsons [30]. We have tested for congruence of the adsorption isotherms with respect to potential of uracil derivatives by preparing plots of ΓRT (calculated by analytical differentiation of fixed potential π versus $\ln a$ curves as described earlier) versus q. Some representative q versus ΓRT plots are shown in fig. 3. It is clear in the case of 1-methyluracil (fig. 3A) that linear q versus ΓRT plots are observed at fixed potentials between −0.3 V and −1.2 V (and, in fact, at even more negative potentials). This implies that for 1-methyluracil the adsorption isotherms are conguent with respect to potential at −0.3 V and more negative

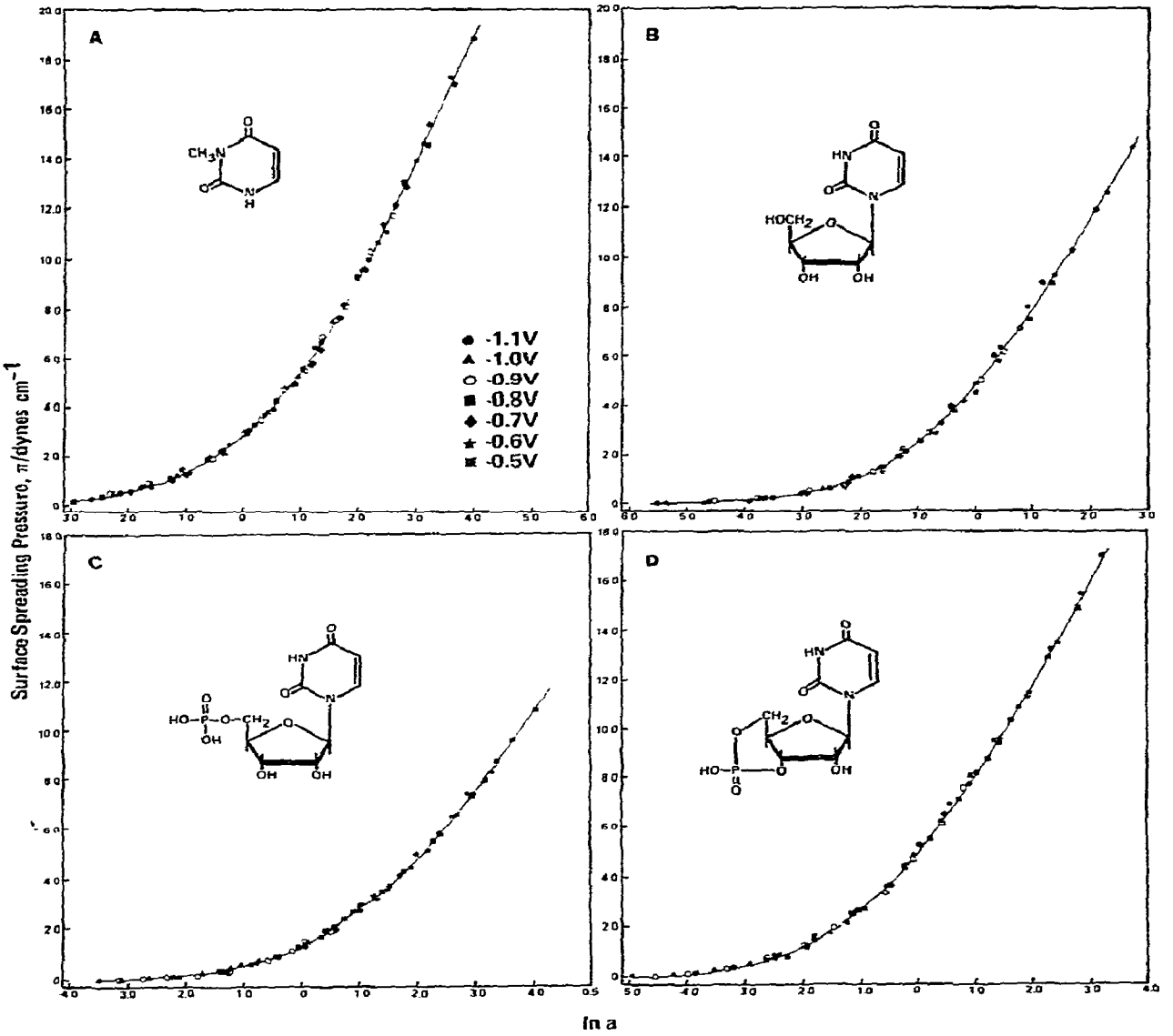

Fig. 2. Composite π versus ln a plots for (A) 3-methyluracil, (B) uridine, (C) uridine-5'-monophosphate and (D) uridine -3',5'-cyclic monophosphate in 0.5 *M* NaF plus 0.01 *M* Na_2HPO_4 pH8. The rms deviation in π from the calculated curve (continuous line) is for (A) 0.198, (B) 0.197, (C) 0.107 and (D) 0.125 dyne cm^{-1}. Data obtained from capacitance results.

potentials. In the case of 1,3-dimethyluracil (fig. 3B) congruence with respect to potential only obtains at potentials more negative than −0.5 V. A summary of the range of potentials over which congruence of the electrosorption isotherms with respect to potential exists for all the uracil derivatives studied is presented

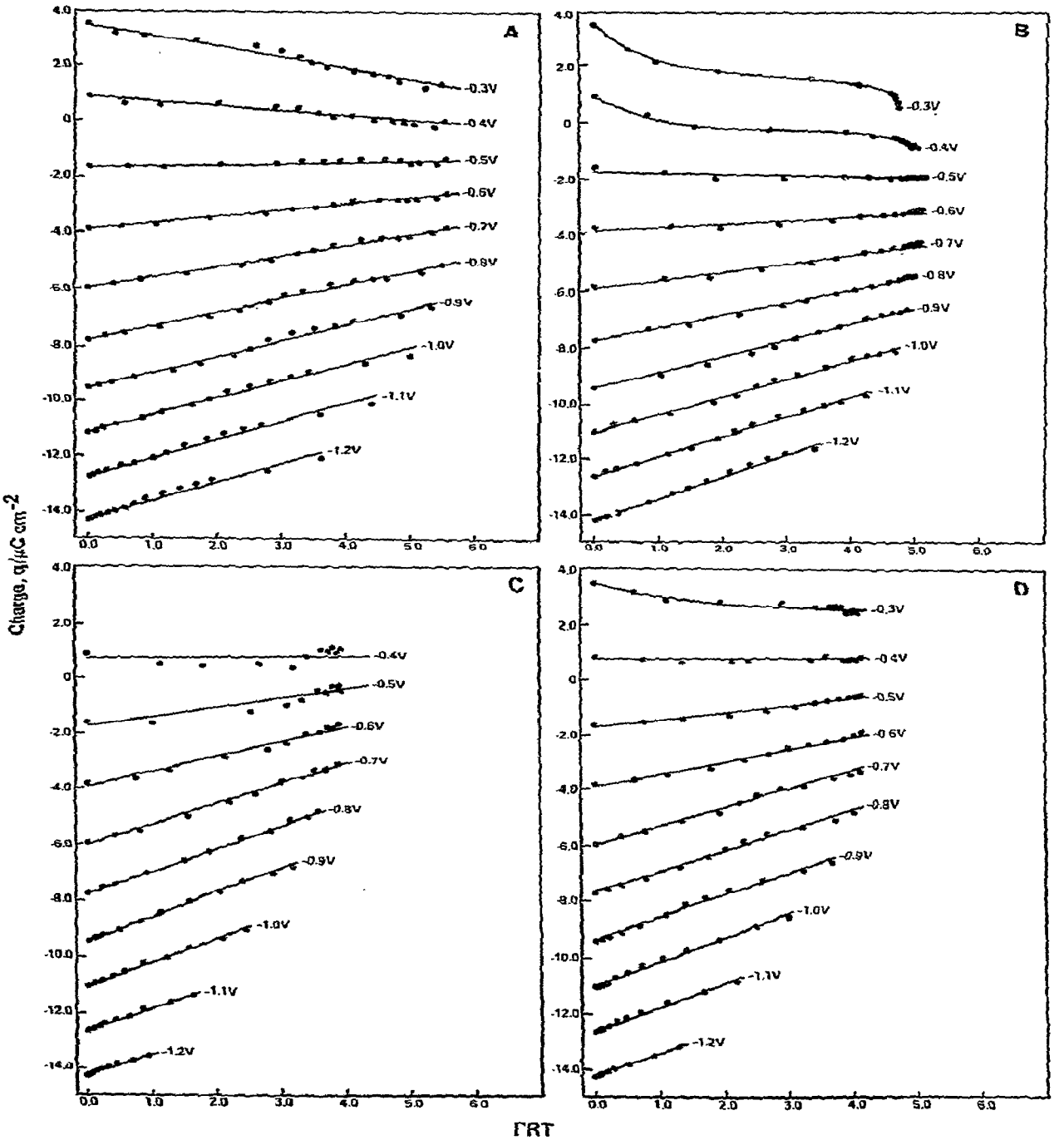

Fig. 3. Test of congruence of electrosorption isotherms with respect to potential for some typical uracil derivatives. (A) 1-Methyluracil, (B) 1,3-dimethyluracil, (C) uridine, and (D) uridine 3',5'-cyclic monophosphate. Supporting electrolyte: 0.5 *M* NaF with 0.01 *M* Na_2HPO_4 buffer pH 8.0. Potential values are indicated in the figure. Data obtained from capacitance results.

Table 1
Range of potentials over wich adsorption isotherms of uracil derivatives are congruent with respect to potential. a)

Compound	Potential range over which congruence exists (Volts versus SCE)
Uracil	−0.3 V to ≥ −1.2
1-Methyluracil	−0.5 to ≥ −1.2
3-Methyluracil	−0.6 to ≥ −1.2
5-Methyluracil (thymine)	−0.4 to ≥ −1.2
1,3-Dimethyluracil	−0.5 to ≥ −1.2
1,5-Dimethyluracil	−0.5 to ≥ −1.2
Uridine	−0.6 to ≥ −1.2
Uridine 5'-monophosphate (UMP)	−0.4 to ≥ −1.2
Uridine 3',5'-cyclic monophosphate (cyclic UMP)	−0.4 to ≥ 1.2

a) Determined from q versus ΓRT plots.

in table 1.

We also tested for the congruence of the adsorption isotherms of uracil derivatives with respect to charge. In this case we prepared plots of E versus ΓRT at fixed charge values. Some typical results are shown in fig. 4. It is clear that in the case of 1-methyluracil (fig. 4A) there is a linear relationship between E and ΓRT over a large range of fixed charge values indicating that the adsorption of this compound is apparently congruent with respect to charge [22]. In the case of 3-methyluracil, however, such a linear relationship between E and ΓRT does not exist (fig. 4B) and hence the isotherms cannot be congruent with respect to charge. A summary of the range of charge values over which congruence of the adsorption isotherms with respect to charge obtains for the various uracil derivatives is shown in table 2.

Comparison of the adsorption results for the uracil derivatives reported here (vide infra) and those obtained for various adenine [20] and thymine [21] systems reveals that for those compounds having C' values (where C' is the capacitance of a completely monolayer covered electrode and is assumed constant [31]) above 12 μF cm^{-2} congruence of adsorption isotherms with respect to charge is noted. The larger the value of C' the greater the range of charge values over which the isotherms exhibit congruence with respect to charge. Thus, uracil has a C' value of 14.28 μF cm^{-2}, the largest observed for any uracil species. This compound exhibits the largest range of charge values for which the congruence condition obtains (see table 2). Damaskin [32] has shown that for organic substances. having relatively large values of C', at relatively low surface activity, simultaneous congruence of adsorption isotherms with respect to both charge and potential can be observed using the above tests.

In view of the fact that the adsorption isotherms of all uracil species are congruent with respect to potential, π, E and a data were fitted to the Frumkin isotherm. The generalized form of the Frumkin isotherm equation is shown in eq. (6).

$$\frac{\theta}{1-\theta} = B_0 a \exp(2\alpha\theta) \exp(-\Phi/\Gamma_m RT) . \qquad (6)$$

In this equation Γ_m is the limiting surface excess of solute at full monolayer coverage in moles cm^{-2}, α is the attraction coefficient and B_0 a constant related to the free energy of adsorption at the ECM potential for the pure supporting electrolyte. The function

$$\Phi = [\gamma_w(0) - \gamma_w(E)] + C'EE_N - C'E^2/2 , \qquad (7)$$

is evaluated in terms of E, the potential relative to the ECM potential for the pure electrolyte, E_N the ECM for the mercury-solution interface at $\theta = 1$, C', and the interfacial tension for the pure supporting electrolyte solution γ_w.

There are two parameters in eq. (7), C' and E_N, and three parameters, α, B_0 and Γ_m in eq. (6) which must be evaluated in fitting data to the generalized Frumkin equation.

By combining the Gibbs equation (eq. 5) with the fixed potential form of the Frumkin equation (eq. 8) and integrating an

$$\frac{\theta}{1-\theta} = Ba \exp(2\alpha\theta) , \qquad (8)$$

equation may be obtained (eq. 9) which directly relates π to α, θ and Γ_m [33].

$$\pi = \Gamma_m RT[-\ln(1-\theta) - \alpha\theta^2] . \qquad (9)$$

A non-linear least squares method has been developed [20] to fit π, E and a data to obtain the best values of the five parameters α, B_0, Γ_m, E_N and C'. Simply, trial values of the 5 parameters are chosen, and values of θ are calculated from eq. (6) for every pair of a and E values by an iterative numerical method. This set of calculated θ_i values is then used to predict a set of π_i

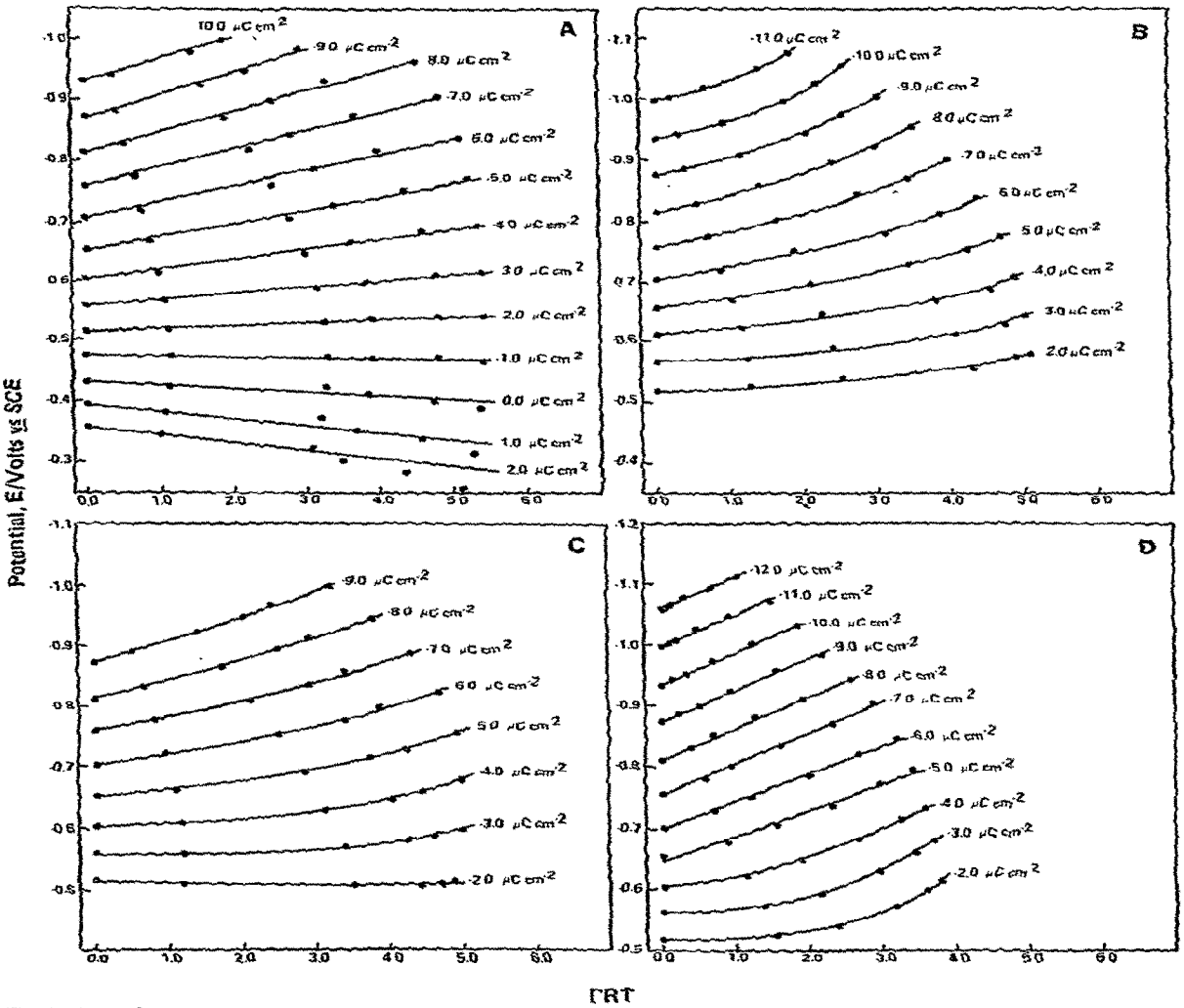

Fig. 4. Tests of congruence of electrosorption isotherms with respect to charge for some typical uracil derivatives. (A) 1-Methyluracil, (B) 3-methyluracil, (C) 1,5-dimethyluracil, (D) uridine. Supporting electrolyte: 0.5 *M* NaF with 0.01 *M* Na_2HPO_4 buffer pH 8.0. Charge values are indicated in the figure. Data obtained from capacitance results.

values using eq. (9). For a given set of parameters a value of the sum of squares of residuals $S = \Sigma_i(\pi_i - \pi_{icalculated})^2$ is obtained and minimized with respect to simultaneous variation of all 5 parameters.

The adherence of the adsorption of various uracil derivatives to the Frumkin model was tested by preparing reduced isotherms. Typical examples, chosen at random, are presented in fig. 5. The experimental ΓRT data in fig. 5 were obtained by analytical differentiation of π versus ln a plots at individual potentials.

Table 2
Range of charge values over which adsorption isotherms of uracil derivatives are congruent with respect to charge. [a]

Compound	Charge range over which congruence exist ($\mu C\ cm^{-2}$)
Uracil	2 to ≥ −12
1-Methyluracil	−1 to −10
3-Methyluracil	NC [b]
5-Methyluracil (*thymine*)	NC
1,3-Dimethyluracil	NC
1,5-Dimethyluracil	NC
Uridine	−5 to −12
Uridine 5'-monophosphate	−1 to −10
Uridine 3',5'-cyclic monophosphate	−3 to −9

a) Determined from E versus ΓRT plots.
b) No congruence at any charge value;

The solid curves are the best fits of all π, E and a data at potentials where the isotherms are congruent with respect to potential as determined by the tests illustrated in fig. 3. The individual experimental points, obtained without assuming any adsorption model, were in all cases in excellent agreement with the Frumkin isotherm. No attempt was made to fit data to other more complex adsorption models because of the excellent fit to the Frumkin model.

Extensive analysis of C versus E data for each uracil derivative in the dilute adsorption region using the Frumkin adsorption model, using the equations and calculational methods outlined earlier, gave the results shown in table 3.

The attraction coefficient, α, is generally very small indicating relatively weak interactions between the adsorbed organic molecules. The ΔG° values at the ECM of the pure supporting electrolyte indicate that uracil has the smallest interaction with the electrode surface. In general, increasing substitution of uracil gives a substantial decrease in ΔG°. The areas occupied by uracil and its methylated derivatives are fairly consistent at 60–70 Å^2. In the case of the ribose or ribosephosphate derivatives of uracil a substantial increase in the area occupied per molecule is observed indicating that the latter substituents occupy a significant fraction of the electrode surface at surface saturation.

The data reported in table 3 were obtained from measurements of double-layer capacitance in the dilute adsorption region. Analysis of π, E and a data obtained from maximum bubble pressure measurements gave very similar results. Some typical examples are shown in table 4.

Table 3
Parameters of the generalized Frumkin isotherm for uracil derivatives determined from capacitance measurements at pH 8.0 [a] in the dilute adsorption region.

Compound	α	$B_0 \times 10^{-3}$ ($l\ mol^{-1}$)	ΔG° [b] (cal)	C' ($\mu F\ cm^{-2}$)	E_N [c] (Volt versus SCE)	Γ_m ($mol\ cm^{-2} \times 10^{10}$)	Area per molecule (Å^2)	rmsd in [d] π ($dyne\ cm^{-1}$)
Uracil	0.45 ± 0.08	0.158 ± 0.005	−2996	14.28 ± 0.38	−0.474 ± 0.003	2.606	64 ± 3	0.156
1-Methyluracil	−0.42 ± 0.09	0.663 ± 0.023	−3847	12.38 ± 0.27	−0.386 ± 0.006	2.337	71 ± 2	0.199
3-Methyluracil	−0.60 ± 0.12	0.831 ± 0.039	−3890	11.74 ± 0.43	−0.400 ± 0.010	2.376	70 ± 3	0.188
5-Methyluracil	0.21 ± 0.04	0.485 ± 0.010	−3667	10.69 ± 0.30	−0.411 ± 0.003	2.922	57 ± 2	0.088
1,3-Dimethyl-uracil	−0.42 ± 0.06	1.709 ± 0.044	−4408	11.05 ± 0.17	−0.309 ± 0.006	2.217	75 ± 1	0.149
1,5-Dimethyl-uracil	0.20 ± 0.08	1.123 ± 0.039	−4159	11.20 ± 0.39	−325.0 ± 0.009	2.332	71 ± 3	0.105
Uridine	−0.008 ± 0.13	4.353 ± 0.327	−4177	14.85 ± 0.50	−0.483 ± 0.009	1.604	104 ± 4	0.181
Uridine 5'-mono phosphate	−0.45 ± 0.12	0.680 ± 0.030	−3863	18.09 ± 0.31	−0.550 ± 0.005	1.382	120 ± 4	0.126
Uridine 3',5'-cyclic phosphate	−0.31 ± 0.08	3.030 ± 0.10	−4156	13.06 ± 0.21	−0.449 ± 0.003	1.732	96 ± 2	0.139

a) 0.5 M NaF plus 0.01 M Na_2HPO_4, pH 8.0. b) $\Delta G = -RT \ln B_0$. c) ECM potential when $\theta = 1.0$. d) Root mean square deviation.

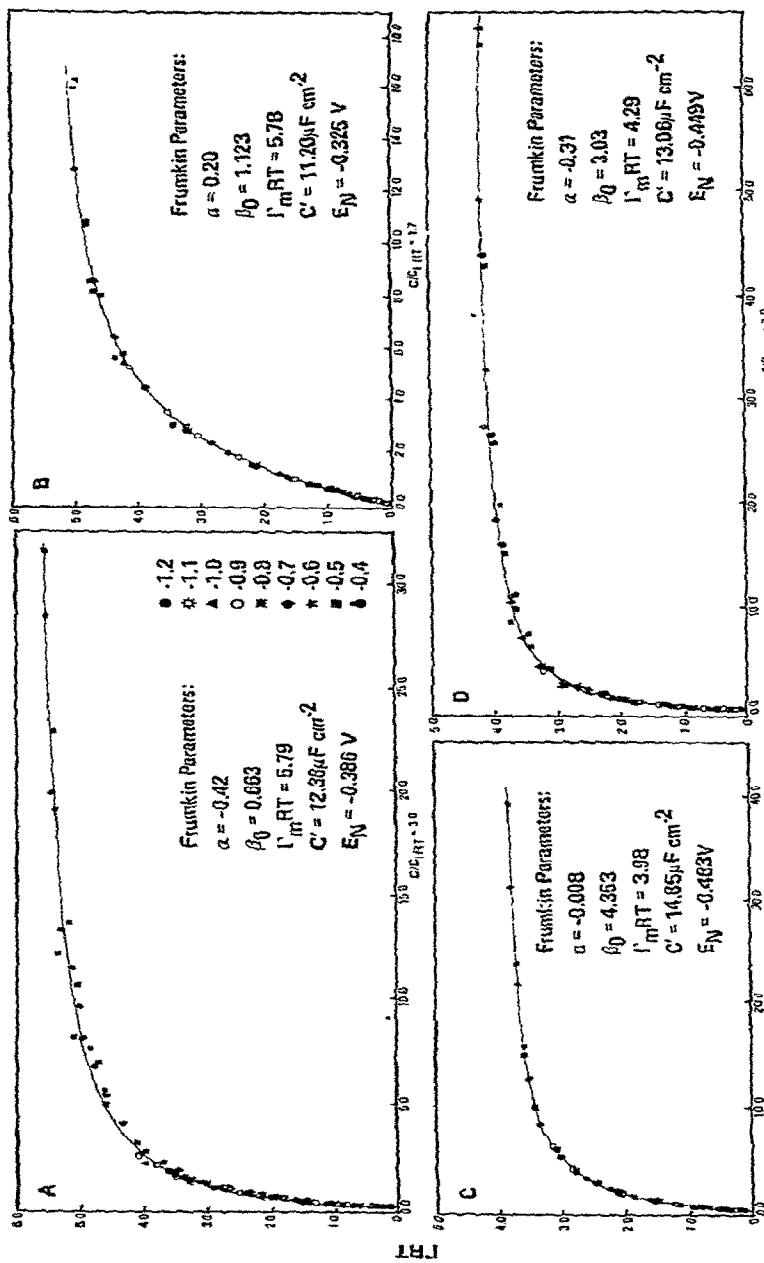

Fig. 5. Reduced adsorption isotherms for (A) 1-methyluracil, (B) 1,5-dimethyluracil, (C) uridine and (D) uridine 3',5'-cyclic monophosphate in the dilute adsorption region in 0.5 *M* NaF plus 0.01 *M* Na_2HPO_4 buffer pH 8.0. The solid line is the best fit of all π, E and a data to the generalized *Frumkin* equation with the values of α, B_0, Γ'_mRT, C' and E_N being shown in the figure. Data obtained from capacitance results.

Table 4

Parameters of the generalized Frumkin isotherm for uracil derivatives determined from maximum bubble pressure measurements at pH 8.0 in the dilute adsorption region

Compound	a	$B_0 \times 10^{-3}$ (l mol^{-1})	ΔG° (cal)	C' (μF cm^{-2})	E_N (Volt versus SCE)	Γ_m (mole cm^{-2} $\times 10^{10}$)	Area per molecule (A^2)	rmsd in π (dyne cm^{-1})
Uracil	0.63 ± 0.09	0.145 ± 0.006	−2945	15.21 ± 0.43	−0.490 ± 0.004	2.630	63 ± 3	0.196
5-Methyluracil	0.81 ± 0.08	0.397 ± 0.016	−3543	14.95 ± 0.35	−0.471 ± 0.004	2.503	66 ± 2	0.215
1,5-Dimethyluracil	0.15 ± 0.09	1.136 ± 0.043	−4166	11.90 ± 0.44	−0.327 ± 0.011	2.363	70 ± 3	0.108

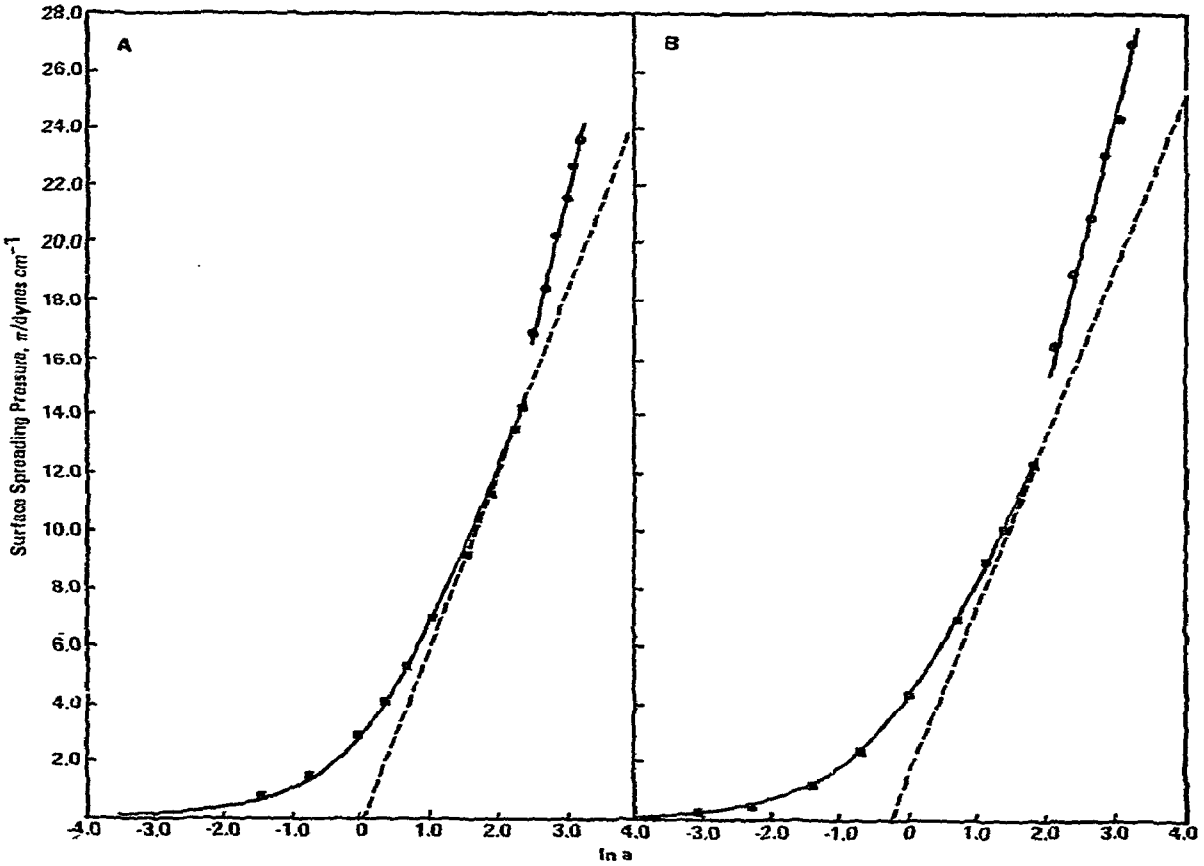

Fig. 6. Surface spreading pressure, π, versus ln a plots for (A) 5-Methyluracil (thymine) and (B) 1,5-dimethyluracil in 0.5 M NaF plus 0.01 M Na_2HPO_4 pH 8.0. Solid squares (■) refer to experimental points obtained at −0.5 V in the dilute adsorption region; solid circles (●) refer to experimental points obtained at −0.5 V at concentrations where the anomalous capacitance pit is observed. Line through solid squares is the best composite π versus ln a fit. Data obtained by the maximum bubble pressure method.

3.3. Capacitance pit region

Using the maximum bubble pressure method it was possible to measure interfacial tension values in both the dilute adsorption region (table 4) and the anomalous capacitance pit region. Only three of the compounds studied, uracil, thymine and 1,5-dimethyluracil, exhibited the capacitance pit; these pits first appeared at 21 mM, 11.0 mM and 6.5 mM concentrations respectively. Using π values obtained from the maximum bubble pressure method it was observed that the π versus ln a curve exhibited a sharp change in slope at concentrations of the uracil species where the capacitance pit was observed. This can be clearly seen in fig. 6 for 5-methyluracil (thymine) and 1,5-dimethyluracil [‡]. Since there is no apparent curvature in the π versus ln a plots in the more steeply sloping region, it may be concluded that θ is virtually unity both in the high concentration range of the dilute adsorption region and in the capacitance pit region. The more steeply sloping region of the π versus ln a curve corresponds to larger Γ_m values or smaller areas occupied by the uracil derivatives than in the dilute adsorption region (table 5). In the case of each compound which exhibits the capacitance pit a decrease of about 40 percent in the area occupied per molecule occurs on passing from virtual surface saturation in the dilute adsorption region to surface saturation in the capacitance pit region. In all cases the area occupied per molecule in the capacitance pit region is about 40 Å^2. This behavior implies, therefore, that at concentrations where these molecules exhibit a capacitance pit a sudden surface reorientation occurs where the area per molecule decreases from 60–70 Å^2 to ca. 40 Å^2.

Table 5
Area occupied per molecule at maximum surface coverage in the dilute and capacitance pit region for various uracil derivatives at pH 8.0 [a,b]

Compound	Area per molecule/Å^2	
	Dilute adsorption region	Capacitance pit region
Uracil	63 ± 3	39.6
5-Methyluracil (thymine)	66 ± 2	39.2
1,5-Dimethyluracil	70 ± 3	42.9

a) 0.5 M NaF plus 0.01 M Na_2HPO_4 pH 8.0
b) Data observed from maximum bubble pressure measurements.

3.4. Surface-orientation of uracil derivatives

In the dilute adsorption region uracil and its methylated derivatives occupy an area ranging from ca. 60–75 Å^2 (see tables 3 and 4). The crystal structure of uracil [34], thymine [35] and related molecules [36] indicates that these molecules are almost planar. Using bond length and bond angle data obtained by X-ray crystallography, and employing van der Waals radii for C, H, N, O of 1.65 Å, 1.2 Å, 1.5 Å and 1.4 Å, respectively, we have calculated that the actual area of uracil is 34 Å^2, thymine is 37 Å^2 and 1,5-dimethyluracil is 41 Å^2. However, it is most unlikely that the individual uracil molecules adsorbed on an electrode surface could pack together and occupy these areas. We have estimated projected areas of 53 Å^2 for uracil [22], 54 Å^2 for thymine and 64 Å^2 for 1,5-dimethyluracil. These areas are quite close to the areas occupied by uracil, mono- and dimethylated uracil derivatives on the mercury electrode surface in the dilute adsorption layer. We have interpreted this to imply that the uracil derivatives are adsorbed flat on the electrode surface in the dilute adsorption layer. The fact that in each instance the area occupied at the electrode-solution interface is slightly larger than the calculated projected area probably indicates that water molecules also occupy a small fraction of the surface. The conclusion that uracil and its methylated derivatives are adsorbed flat on the electrode surface is in accord with recent reports on other purines and pyrimidines [20–23].

At concentrations where uracil, thymine and 1,5-dimethyluracil give rise to a capacitance pit the area occupied decreases in all cases by about 40 percent. We believe that the only reasonable explanation of this effect is that the uracil species adsorbed flat on the electrode in the dilute adsorption region reorients and then stands in a perpendicular orientation on the electrode surface. Once in a perpendicular surface orientation the various uracil derivatives would be expected to undergo extensive vertical stacking interactions [37]. That this is so is borne out by the fact that of the three compounds which exhibit the capacitance pit (table 5), i.e., undergo a surface reorientation pro-

[‡] Similar curves for uracil have been presented elsewhere [22].

cess, increasing methylation decreases the concentration necessary to observe the reorientation process. Thus, a bulk-solution concentration of 6.5 m*M* is required to observe the capacitance pit for 1,5-dimethyluracil. In the case of thymine and uracil the corresponding concentrations are 11 m*M* and 21 m*M* respectively.

The suggestion that uracil, thymine and 1,5-dimethyluracil adopt a perpendicular orientation is supported by the large decrease in area occupied by each species in the capacitance pit region. The area that one might theoretically expect uracil and 5-methyluracil to occupy when in a perpendicular orientation may be approximated from molar volume (MW/density) values. The density of uracil is 1.617 g cm^{-3} [47] while that for 5-methyluracil is 1.454 g cm^{-3} [35]. Hence, the molar volume of uracil is 69.26 cm^3 and of 5-methyluracil is 86.66 cm^3 which corresponds to molecular volumes of 115 $Å^3$ and 144 $Å^3$, respectively. The approximate thickness of uracil is hence (molecular volume/absolute molecular area) 3.4 Å while for 5-methyluracil the thickness is 3.9 Å. Calculations hence reveal that the area occupied by uracil in the perpendicular stance is ≈ 26 $Å^2$ while that for 5-methyluracil is 29 $Å^2$. Density data for 1,5-dimethyluracil are not available but a reasonable estimate of its area in a perpendicular orientation bound through the N(3) or N(1) hydrogens (vide infra) is ≈ 33 $Å^2$. These areas are a little smaller than the experimental areas of 39–43 $Å^2$ (table 5). It would seem logical, however, that water molecules would occupy any electrode surface not filled by uracil molecules.

It has been found that generally only those purines or pyrimidines found naturally in nucleic acids exhibit anomalous capacitance pits, at least at relatively low concentrations [22–24,38–41]. Of the compounds examined in this study, uracil and thymine are both naturally occurring nucleic acid components, and both give the capacitance pit. On the other hand, 1,5-dimethyluracil occurs only occasionally in nucleic acids [42]. However, the preponderance of purines and pyrimidines that give the capacitance pit are common components of nucleic acids. This has led us to believe that the structural functionalities associated with hydrogen bonding of complementary bases in nucleic acids are, at least in part, responsible for binding to the electrode surface when these molecules are in their perpendicular surface orientation. In the case of uracil hydrogen-bonding to adenine in nucleic acid occurs as shown below. This would suggest that the hydrogen at N(3) or uracil or thymine is responsible

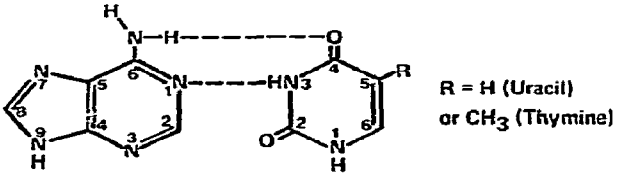

for binding to the electrode when these molecules adopt a perpendicular surface orientation corresponding to the capacitance pit. This idea is supported by the fact that methylation at N(3) destroys the ability of uracil to adopt a perpendicular orientation. However, 1-methyluracil also fails to adopt a perpendicular surface orientation. This suggests that not only the hydrogen at N(3) is capable of binding uracil to the electrode but also the hydrogen at N(1), i.e., there are two binding sites for uracil when it adopts a perpendicular surface orientation. Methylation at C(5) enhances the ability of uracil to adopt a perpendicular surface orientation; i.e., the capacitance pit occurs at 11 m*M* for thymine compared to 21 m*M* for uracil. Surprisingly, however, 1,5-dimethyluracil exhibits a capacitance pit, or perpendicular orientation, at the lowest concentration of all uracil derivatives, 6.5 m*M*.

When any of the three uracil derivatives that exhibit a capacitance pit are in a perpendicular surface stance they must undergo stacking interactions similar to those observed in nucleic acids or in aqueous solution(s). It is also a well-accepted fact that methylation of pyrimidines enhances the association or base stacking tendency [37].

Thus, in order to explain the ability of uracil and its derivatives to adopt a perpendicular surface orientation, it appears that at least three factors must be considered. These are: (a) the number of binding sites available, i.e., N(1)H and N(3)H; (b) the strength of interaction between the uracil derivative in its flat orientation (dilute adsorption region) and the electrode surface, i.e., ΔG° (table 3) and, (c) the effect of ring substituents on enhancing stacking interactions when the molecules reorient to a perpendicular stance.

Thus, methylation of uracil at N(1) or N(3) removes a perpendicular binding site and increases the degree of interaction between the organic molecule and the electrode surface; i.e., ΔG° is almost 900 cal more negative in the case of 1- or 3-methyluracil than for uracil

(table 3). These two effects must more than compensate for the effect of the N-methyl group, which should enhance the stacking interactions if the molecule could adopt a perpendicular orientation. In the case of 1,3-dimethyluracil both perpendicular binding sites are blocked and there is no possibility for the molecule to adopt a perpendicular surface orientation.

For 5-methyluracil (thymine) both perpendicular binding sites are available and the 5-methyl group would be expected to increase the stacking interactions of the molecules. Both of these effects would favor thymine being capable of adopting a perpendicular surface orientation. The single methyl group, however, increases the interaction of the molecule in its flat orientation with the electrode surface compared to uracil (see table 3). The latter effect must be less important than the combined effect of the presence of two perpendicular binding sites, and increased stacking interaction resulting from the substituted methyl group. The overall result is that thymine not only can adopt a perpendicular surface orientation, but it does so at a significantly lower concentration than uracil.

In the case of 1,5-dimethyluracil, similar arguments may be applied. Thus, acting to inhibit the perpendicular surface orientation of this molecule is the loss of one perpendicular binding site and (compared to uracil) an increased interaction between the molecule in its flat orientation and the electrode. Apparently, the extra stacking interaction caused by the presence of two substituent methyl groups more than compensates for the two latter effects so that 1,5-dimethyluracil adopts a perpendicular orientation at lower concentrations (6.5 m*M*) than any other uracil species.

Uridine, UMP and cyclic UMP exhibit no tendency to adopt a perpendicular surface orientation. The larger areas occupied by these molecules compared to uracil suggest that not only is the uracil residue adsorbed flat on the electrode but also the ribose or ribosephosphate occupies a significant amount of the surface. The failure of uridine to adopt a perpendicular surface orientation can be explained by similar reasoning. Thus, a perpendicular binding site is occupied by a ribose residue, and the interaction with the electrode between the flat oriented uridine molecule is greater than for uracil (table 3). Finally, the ribose substituent, being electron withdrawing [43–45], would be expected to decrease the stacking interaction between perpendicular base units if uracil could adopt such a configuration. Although not widely investigated, there is evidence that even in homogeneous solution a nucleoside, such as purine riboside, exhibits less stacking tendency than the free base [46], which supports the latter conclusion. In the case of the nucleotides of uracil the extensive ionization of these compounds would result in extensive repulsive interactions for molecules in a perpendicular orientation which would act to prevent such orientations occurring.

3.5. Conclusions

The results reported here appear to support the view that uracil and its mono- and dimethylated derivatives are adsorbed first in a region, called the dilute adsorption region, where the essentially planar molecules are adsorbed in a flat orientation on the electrode surface (i.e., parallel to the electrode surface) over a wide range of potentials. The same situation seems to prevail for uridine, uridine-5'-monophosphate and uridine-3',5'-cyclic monophosphate, i.e., the uracil residue is adsorbed flat on the electrode. However, the ribose or ribosephosphate is also adsorbed on the electrode surface.

In the case of uracil, thymine and 1,5-dimethyluracil, a surface reorientation process takes place at critical values of bulk-solution concentration and electrode potential. The molecules reorient from a flat orientation to a perpendicular orientation with respect to the electrode surface. In the perpendicular orientation these uracil derivatives are bound to the electrode surface though the N(3)-H or perhaps N(1)-H groups in a hydrogen bonding-like model perhaps as illustrated in fig. 7. When in the perpendicular mode appreciable

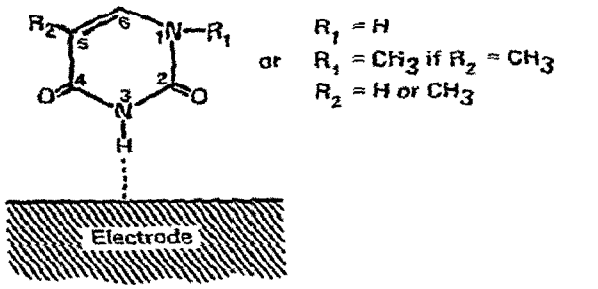

Fig. 7. Possible mode of binding of uracil derivatives to the electrode surface when in a perpendicular surface orientation.

stacking interactions (association) between adjacent molecules must occur similar to those observed between adjacent bases in nucleic acids giving rose to a very compact surface film.

References

[1] A.A. Pilla, Bioelectrochem. Bioenergetics 1 (1974) 227.
[2] F.W. Cope, Bull. Math. Biophys. 25 (1963) 165; 27 (1965) 237.
[3] F.W. Cope, Arch. Biochem. Biophys. 103 (1963) 352.
[4] F.W. Cope, J. Chem. Phys. 40 (1964) 2653.
[5] F.W. Cope, Experientia Suppl. 18 (1971) 223.
[6] F.W. Cope and K.D. Straub, Bull. Math. Biophys. 31 (1969) 761.
[7] F.W. Cope, Adv. Biol. Med. Phys. 13 (1970) 1.
[8] S. Eisenberg, S. Ben-or and F. Doljanski, Exptl. Cell Res. 26 (1962) 451.
[9] E. Mayhew and L. Weiss, Expl. Cell Res. 50 (1968) 441.
[10] E. Mayhew, J. Gen. Physiol. 49 (1966) 717.
[11] T.P. Brent and J.A. Forrester, Nature 215 (1967) 92.
[12] R.O. Becker, J. Bone Joint Surg. 43A (1961) 643.
[13] R.O. Becker and D.G. Murray, Clin. Ortho. 75 (1970) 1969.
[14] T.L. Hill, J. Amer. Chem. Soc. 80 (1958) 2142.
[15] C.T. O'Konski and N.C. Stellwagen, Biophys. J. 5 (1965) 607.
[16] E. Neumann and A. Katchalsky, Proc. Nat. Acad. Sci. U.S.A. 69 (1972) 993.
[17] A.V. Field, A.A. Tytell, P.G. Lampson and M.R. Hilleman, Proc. Nat. Acad. Sci., U.S.A. 58 (1967) 1004.
[18] P.L. Schell, Biochim. Biophys. Acta 240 (1971) 472.
[19] V. Brabec and E. Paleček, Biophys. Chem. 4 (1976) 79.
[20] H. Kinoshita, S.D. Christian and G. Dryhurst, J. Electroanal. Chem. Interfac. Electrochem., 83 (1977) 151.
[21] H. Kinoshita, S.D. Christian and G. Dryhurst, J. Electroanal. Chem. Interfac. Electrochem., in press.
[22] V. Brabec, S.D. Christian and G. Dryhurst, J. Electroanal. Chem. Interfac. Electrochem., in press.
[23] H. Kinoshita, S.D. Christian, M.H. Kim, J.G. Baker and G. Dryhurst, American Chemical Society Symposium Series on Electrochemical Studies of Biological Systems, Ed. D.T. Sawyer, 38 (1977) 113.
[24] G. Dryhurst and P.J. Elving, Talanta 16 (1969) 855.
[25] D.E. Broadhead, R.S. Hansen and G.W. Potter, J. Colloi Interface Sci. 31 (1969) 61.
[26] D.C. Grahame, E.M. Coffin, J.P. Cummings and M.A. Poth, J. Amer. Chem. Soc. 74 (1952) 1207.
[27] J. Lawrence, R. Parsons and R. Payne, J. Electroanal. Chem. Interfac. Electrochem. 16 (1968) 193.
[28] D.J. Schiffrin, J. Electroanal, Chem. Interfac. Electrochem. 23 (1969) 168.
[29] Our computational method employs an optimizing program, written by Dr. E. Enwall, incorporating an algorithm given by D.W. Marquardt, J. Soc. Indust. App Math. 11 (1963) 431.
[30] R. Parsons, J. Electroanal. Chem. Interfac. Electrochem. 8 (1964) 93.
[31] B.B. Damaskin, O.A. Petrii and V. Batrakov, Adsorptior of organic compounds on electrodes (Plenum, New Yorl 1971) p. 112.
[32] B.B. Damaskin, Elektrokhimiya, 11 (1975) 428.
[33] D.E. Broadhead, K.G. Baikerikar and R.S. Hansen, J. Phys. Chem. 80 (1976) 370.
[34] R.F. Stewart and L.H. Jensen, Acta cryst. 23 (1967) 1102.
[35] R. Gerdil, Acta Cryst. 14 (1961) 333.
[36] J. Donohue, Arch. Biochem. Biophys. 128 (1968) 591.
[37] P.O.P. Ts'o, in Molecular Associations in Biology, B. Pullman (Ed.) Academic, New York, 1968, p. 39.
[38] V. Vetterl, Coll. Czech. Chem. Commun. 31 (1966) 2105.
[39] V. Vetterl, J. Electroanal. Chem. Interfac. Electrochem. 19 (1968) 169.
[40] V. Vetterl, Abh. Deut. Wiss. Berlin, Kl. Med. (1966) 493.
[41] V. Vetterl, Biophysik, 5 (1968) 255.
[42] J.H. Spencer, The physics and chemistry of DNA and RNA (W.B. Saunders, Philadelphia, 1972) p. 19.
[43] C.D. Jardetzky and O. Jardetzky, J. Am. Chem. Soc. 82 (1960) 222.
[44] J. Clauwaert and J. Stockx, Z. Naturforsch, B23 (1968) 25.
[45] M.P. Schweizer, A.D. Broom, P.O.P. Ts'o and D.P. Hollis J. Am. Chem. Soc. 90 (1968) 1042.
[46] A.D. Broom, M.P. Schweizer, P.O.P. Ts'o, J. Am. Chem. Soc. 89 (1967) 3612.
[47] G.S. Parry, Acta Crust. 7 (1954) 313.